

Observing Application

Date: Aug 01, 2018
Proposal ID: GBT/19A-240
Legacy ID: QL269
PI: Lukas Leisman
Type: Regular
Category: Extragalactic Structure
Total time: 49.5

HI Observations of Very Low Surface Brightness Galaxies from the HSC Survey

Abstract:

We propose to observe the HI in 56 very low surface brightness galaxies (vLSBs) that were detected in the Hyper Suprime-Cam Subaru Strategic Program. vLSBs are a cosmologically significant population of galaxies, yet are not well understood: such galaxies appear to have effective radii similar to the Milky Way, yet very small stellar masses. To date, only 8 of the 781 vLSBs in the Hyper Suprime-Cam sample have measured distances. Our goal is to determine redshift distances to a carefully selected subset of vLSB galaxies likely to have HI and to be in the field. Based on HI scaling relations, we expect to detect roughly 70% of our targets. This represents nearly a five-fold increase in the number of known redshifts for such galaxies with a modest investment of observing time compared with optical spectroscopy. In addition, HI gas fractions and masses will be used to probe their star formation histories and line widths will be used to probe rotation and dark matter content. These measurements will constrain the cosmic number density and formation models for this enigmatic population of vLSB galaxies in low density environments.

Authors:

Name	Institution	Email	Status
Leisman, Lukas	Valparaiso University	luke.leisman@valpo.edu	
Greco, Johnny	Ohio State University	greco.40@osu.edu	
Hallenbeck, Gregory	Union College	hallenbg@union.edu	
Pisano, D.J.	West Virginia University	djpisano@mail.wvu.edu	
Greene, Jenny	Princeton University	jgreene@astro.princeton.edu	
Haynes, Martha	Cornell University	haynes@astro.cornell.edu	
Koopmann, Rebecca	Union College	koopmanr@union.edu	
Ribaudo, Joseph	Utica College	jsribaudo@utica.edu	
Craig, David	West Texas A&M University	dcraig@wtamu.edu	
Denn, Grant	Denver, Metropolitan State University of	gdenn@msudenver.edu	
O'Donoghue, Aileen	St. Lawrence University	aodonoghue@stlawu.edu	
Durbala, Adriana	Wisconsin-Stevens Point, University of	adurbala@uwsp.edu	
Goulding, Andy	Princeton University	goulding@astro.princeton.edu	
Huang, Song	California at Santa Cruz, University of	shuang89@ucsc.edu	

Name	Institution	Email	Status
Rabidoux, Katherine	University of Wisconsin-Platteville	rabidouxk@uwplatt.edu	
Rosenberg, Jessica	George Mason University	jrosenb4@gmu.edu	
Smith, Evan	West Virginia University	etsmit12@gmail.com	
Strauss, Michael	Princeton University	strauss@astro.princeton.edu	

Principal Investigator: Lukas Leisman
 Contact: Lukas Leisman
 Telephone: 6163409353
 Email: luke.leisman@valpo.edu

Related Proposals:

Joint:

Not a Joint Proposal.

Observing type(s):

Spectroscopy

GBT Resources

Name	Group	Frontend & Backend	Setup
Redshifted HI	Observation Mode	L-Band (1.15-1.73 GHz) VEGAS	Observing type: Spectral Line Number of beams: 1 Number of spectrometers: 1

Spectrometer #	1
Mode	8
Bandwidth (MHz)	100.0
Rest frequencies (GHz)	1.380
Spectral resolution (KHz)	1.5
Integration time (s)	5.0
Data rate (MB/s)	0.2

Sources

Name	Position		Velocity		Group
6	Coordinate system	Equatorial	Convention	Optical	targets
	Equinox	J2000			
	Right Ascension	16:17:56.0	Ref. frame	Barycentric	
		00:00:00			
	Declination	+44:17:25.8	Velocity	0	
		00:00:00			
Calibrator	No				

Name	Position		Velocity		Group
8	Coordinate system	Equatorial	Convention	Optical	targets
	Equinox	J2000			
	Right Ascension	16:09:11.1	Ref. frame	Barycentric	
		00:00:00			
	Declination	+44:21:31.8	Velocity	0	
00:00:00					
Calibrator	No				
19	Coordinate system	Equatorial	Convention	Optical	targets
	Equinox	J2000			
	Right Ascension	16:19:05.7	Ref. frame	Barycentric	
		00:00:00			
	Declination	+41:58:16.5	Velocity	0	
00:00:00					
Calibrator	No				
25	Coordinate system	Equatorial	Convention	Optical	targets
	Equinox	J2000			
	Right Ascension	16:19:21.3	Ref. frame	Barycentric	
		00:00:00			
	Declination	+42:15:01.6	Velocity	0	
00:00:00					
Calibrator	No				
29	Coordinate system	Equatorial	Convention	Optical	targets
	Equinox	J2000			
	Right Ascension	16:12:45.6	Ref. frame	Barycentric	
		00:00:00			
	Declination	+42:47:41.2	Velocity	0	
00:00:00					
Calibrator	No				
36	Coordinate system	Equatorial	Convention	Optical	targets
	Equinox	J2000			
	Right Ascension	15:57:07.8	Ref. frame	Barycentric	
		00:00:00			
	Declination	+42:09:23.6	Velocity	0	
00:00:00					
Calibrator	No				
39	Coordinate system	Equatorial	Convention	Optical	targets
	Equinox	J2000			
	Right Ascension	15:48:10.5	Ref. frame	Barycentric	
		00:00:00			
	Declination	+43:09:24.4	Velocity	0	
00:00:00					
Calibrator	No				

Name	Position		Velocity		Group
40	Coordinate system	Equatorial	Convention	Optical	targets
	Equinox	J2000			
	Right Ascension	15:46:57.9	Ref. frame	Barycentric	
		00:00:00			
	Declination	+42:35:50.0	Velocity	0	
00:00:00					
Calibrator	No				
394	Coordinate system	Equatorial	Convention	Optical	targets
	Equinox	J2000			
	Right Ascension	09:00:19.1	Ref. frame	Barycentric	
		00:00:00			
	Declination	+03:42:19.1	Velocity	0	
00:00:00					
Calibrator	No				
405	Coordinate system	Equatorial	Convention	Optical	targets
	Equinox	J2000			
	Right Ascension	09:09:21.4	Ref. frame	Barycentric	
		00:00:00			
	Declination	+01:49:40.7	Velocity	0	
00:00:00					
Calibrator	No				
407	Coordinate system	Equatorial	Convention	Optical	targets
	Equinox	J2000			
	Right Ascension	09:01:33.8	Ref. frame	Barycentric	
		00:00:00			
	Declination	+02:20:14.3	Velocity	0	
00:00:00					
Calibrator	No				
412	Coordinate system	Equatorial	Convention	Optical	targets
	Equinox	J2000			
	Right Ascension	08:47:40.7	Ref. frame	Barycentric	
		00:00:00			
	Declination	+02:30:02.7	Velocity	0	
00:00:00					
Calibrator	No				
421	Coordinate system	Equatorial	Convention	Optical	targets
	Equinox	J2000			
	Right Ascension	08:39:45.5	Ref. frame	Barycentric	
		00:00:00			
	Declination	+01:51:25.4	Velocity	0	
00:00:00					
Calibrator	No				

Name	Position		Velocity		Group
422	Coordinate system	Equatorial	Convention	Optical	targets
	Equinox	J2000			
	Right Ascension	14:57:43.3	Ref. frame	Barycentric	
		00:00:00			
	Declination	+01:21:18.6	Velocity	0	
00:00:00					
Calibrator	No				
438	Coordinate system	Equatorial	Convention	Optical	targets
	Equinox	J2000			
	Right Ascension	15:02:07.7	Ref. frame	Barycentric	
		00:00:00			
	Declination	+01:30:56.7	Velocity	0	
00:00:00					
Calibrator	No				
468	Coordinate system	Equatorial	Convention	Optical	targets
	Equinox	J2000			
	Right Ascension	14:21:07.9	Ref. frame	Barycentric	
		00:00:00			
	Declination	+00:53:06.3	Velocity	0	
00:00:00					
Calibrator	No				
481	Coordinate system	Equatorial	Convention	Optical	targets
	Equinox	J2000			
	Right Ascension	13:59:36.6	Ref. frame	Barycentric	
		00:00:00			
	Declination	+00:47:30.3	Velocity	0	
00:00:00					
Calibrator	No				
483	Coordinate system	Equatorial	Convention	Optical	targets
	Equinox	J2000			
	Right Ascension	12:13:36.6	Ref. frame	Barycentric	
		00:00:00			
	Declination	+00:41:28.0	Velocity	0	
00:00:00					
Calibrator	No				
495	Coordinate system	Equatorial	Convention	Optical	targets
	Equinox	J2000			
	Right Ascension	12:06:31.5	Ref. frame	Barycentric	
		00:00:00			
	Declination	+01:28:50.5	Velocity	0	
00:00:00					
Calibrator	No				

Name	Position		Velocity		Group
496	Coordinate system	Equatorial	Convention	Optical	targets
	Equinox	J2000			
	Right Ascension	12:06:30.0	Ref. frame	Barycentric	
		00:00:00			
	Declination	+01:33:22.7	Velocity	0	
00:00:00					
Calibrator	No				
497	Coordinate system	Equatorial	Convention	Optical	targets
	Equinox	J2000			
	Right Ascension	12:08:07.2	Ref. frame	Barycentric	
		00:00:00			
	Declination	+00:52:04.8	Velocity	0	
00:00:00					
Calibrator	No				
515	Coordinate system	Equatorial	Convention	Optical	targets
	Equinox	J2000			
	Right Ascension	12:05:14.6	Ref. frame	Barycentric	
		00:00:00			
	Declination	+01:46:09.5	Velocity	0	
00:00:00					
Calibrator	No				
522	Coordinate system	Equatorial	Convention	Optical	targets
	Equinox	J2000			
	Right Ascension	12:04:46.3	Ref. frame	Barycentric	
		00:00:00			
	Declination	+01:17:54.2	Velocity	0	
00:00:00					
Calibrator	No				
527	Coordinate system	Equatorial	Convention	Optical	targets
	Equinox	J2000			
	Right Ascension	11:54:43.5	Ref. frame	Barycentric	
		00:00:00			
	Declination	+01:39:07.6	Velocity	0	
00:00:00					
Calibrator	No				
538	Coordinate system	Equatorial	Convention	Optical	targets
	Equinox	J2000			
	Right Ascension	09:22:35.2	Ref. frame	Barycentric	
		00:00:00			
	Declination	+01:31:23.3	Velocity	0	
00:00:00					
Calibrator	No				

Name	Position		Velocity		Group
540	Coordinate system	Equatorial	Convention	Optical	targets
	Equinox	J2000			
	Right Ascension	09:18:55.4	Ref. frame	Barycentric	
		00:00:00			
	Declination	+01:45:05.7	Velocity	0	
00:00:00					
Calibrator	No				
548	Coordinate system	Equatorial	Convention	Optical	targets
	Equinox	J2000			
	Right Ascension	08:55:30.4	Ref. frame	Barycentric	
		00:00:00			
	Declination	+00:50:44.3	Velocity	0	
00:00:00					
Calibrator	No				
559	Coordinate system	Equatorial	Convention	Optical	targets
	Equinox	J2000			
	Right Ascension	08:47:16.9	Ref. frame	Barycentric	
		00:00:00			
	Declination	+01:37:20.8	Velocity	0	
00:00:00					
Calibrator	No				
573	Coordinate system	Equatorial	Convention	Optical	targets
	Equinox	J2000			
	Right Ascension	08:36:48.0	Ref. frame	Barycentric	
		00:00:00			
	Declination	+01:21:24.8	Velocity	0	
00:00:00					
Calibrator	No				
589	Coordinate system	Equatorial	Convention	Optical	targets
	Equinox	J2000			
	Right Ascension	14:39:50.9	Ref. frame	Barycentric	
		00:00:00			
	Declination	+00:21:11.1	Velocity	0	
00:00:00					
Calibrator	No				
593	Coordinate system	Equatorial	Convention	Optical	targets
	Equinox	J2000			
	Right Ascension	14:35:30.0	Ref. frame	Barycentric	
		00:00:00			
	Declination	-00:18:40.8	Velocity	0	
00:00:00					
Calibrator	No				

Name	Position		Velocity		Group
603	Coordinate system	Equatorial	Convention	Optical	targets
	Equinox	J2000			
	Right Ascension	14:20:05.0	Ref. frame	Barycentric	
		00:00:00			
	Declination	-00:26:09.0	Velocity	0	
00:00:00					
Calibrator	No				
605	Coordinate system	Equatorial	Convention	Optical	targets
	Equinox	J2000			
	Right Ascension	14:16:09.6	Ref. frame	Barycentric	
		00:00:00			
	Declination	-00:23:20.1	Velocity	0	
00:00:00					
Calibrator	No				
612	Coordinate system	Equatorial	Convention	Optical	targets
	Equinox	J2000			
	Right Ascension	14:06:40.1	Ref. frame	Barycentric	
		00:00:00			
	Declination	+00:08:50.6	Velocity	0	
00:00:00					
Calibrator	No				
613	Coordinate system	Equatorial	Convention	Optical	targets
	Equinox	J2000			
	Right Ascension	14:06:36.8	Ref. frame	Barycentric	
		00:00:00			
	Declination	+00:03:55.7	Velocity	0	
00:00:00					
Calibrator	No				
614	Coordinate system	Equatorial	Convention	Optical	targets
	Equinox	J2000			
	Right Ascension	14:06:17.3	Ref. frame	Barycentric	
		00:00:00			
	Declination	+00:37:46.0	Velocity	0	
00:00:00					
Calibrator	No				
621	Coordinate system	Equatorial	Convention	Optical	targets
	Equinox	J2000			
	Right Ascension	12:00:40.2	Ref. frame	Barycentric	
		00:00:00			
	Declination	+00:33:49.1	Velocity	0	
00:00:00					
Calibrator	No				

Name	Position		Velocity		Group
623	Coordinate system	Equatorial	Convention	Optical	targets
	Equinox	J2000			
	Right Ascension	12:00:17.3	Ref. frame	Barycentric	
		00:00:00			
	Declination	+00:33:43.2	Velocity	0	
00:00:00					
Calibrator	No				
625	Coordinate system	Equatorial	Convention	Optical	targets
	Equinox	J2000			
	Right Ascension	12:01:06.5	Ref. frame	Barycentric	
		00:00:00			
	Declination	+00:14:34.2	Velocity	0	
00:00:00					
Calibrator	No				
629	Coordinate system	Equatorial	Convention	Optical	targets
	Equinox	J2000			
	Right Ascension	11:55:50.8	Ref. frame	Barycentric	
		00:00:00			
	Declination	+00:04:53.7	Velocity	0	
00:00:00					
Calibrator	No				
659	Coordinate system	Equatorial	Convention	Optical	targets
	Equinox	J2000			
	Right Ascension	08:44:53.5	Ref. frame	Barycentric	
		00:00:00			
	Declination	-00:15:42.6	Velocity	0	
00:00:00					
Calibrator	No				
705	Coordinate system	Equatorial	Convention	Optical	targets
	Equinox	J2000			
	Right Ascension	14:17:46.2	Ref. frame	Barycentric	
		00:00:00			
	Declination	-00:43:21.4	Velocity	0	
00:00:00					
Calibrator	No				
716	Coordinate system	Equatorial	Convention	Optical	targets
	Equinox	J2000			
	Right Ascension	14:09:43.7	Ref. frame	Barycentric	
		00:00:00			
	Declination	-1:51:32.0	Velocity	0	
00:00:00					
Calibrator	No				

Name	Position		Velocity		Group
722	Coordinate system	Equatorial	Convention	Optical	targets
	Equinox	J2000			
	Right Ascension	14:04:42.0	Ref. frame	Barycentric	
		00:00:00			
	Declination	-1:22:27.3	Velocity	0	
00:00:00					
Calibrator	No				
728	Coordinate system	Equatorial	Convention	Optical	targets
	Equinox	J2000			
	Right Ascension	14:05:03.6	Ref. frame	Barycentric	
		00:00:00			
	Declination	-00:41:54.8	Velocity	0	
00:00:00					
Calibrator	No				
731	Coordinate system	Equatorial	Convention	Optical	targets
	Equinox	J2000			
	Right Ascension	13:58:51.5	Ref. frame	Barycentric	
		00:00:00			
	Declination	-00:53:28.2	Velocity	0	
00:00:00					
Calibrator	No				
741	Coordinate system	Equatorial	Convention	Optical	targets
	Equinox	J2000			
	Right Ascension	12:01:40.5	Ref. frame	Barycentric	
		00:00:00			
	Declination	-1:12:15.6	Velocity	0	
00:00:00					
Calibrator	No				
745	Coordinate system	Equatorial	Convention	Optical	targets
	Equinox	J2000			
	Right Ascension	12:04:55.6	Ref. frame	Barycentric	
		00:00:00			
	Declination	-00:41:44.4	Velocity	0	
00:00:00					
Calibrator	No				
748	Coordinate system	Equatorial	Convention	Optical	targets
	Equinox	J2000			
	Right Ascension	11:58:16.7	Ref. frame	Barycentric	
		00:00:00			
	Declination	-1:29:21.2	Velocity	0	
00:00:00					
Calibrator	No				

Name	Position		Velocity		Group
750	Coordinate system	Equatorial	Convention	Optical	targets
	Equinox	J2000			
	Right Ascension	11:59:43.6	Ref. frame	Barycentric	
		00:00:00			
	Declination	-00:46:21.8	Velocity	0	
00:00:00					
Calibrator	No				
765	Coordinate system	Equatorial	Convention	Optical	targets
	Equinox	J2000			
	Right Ascension	11:44:33.8	Ref. frame	Barycentric	
		00:00:00			
	Declination	-00:52:00.4	Velocity	0	
00:00:00					
Calibrator	No				
766	Coordinate system	Equatorial	Convention	Optical	targets
	Equinox	J2000			
	Right Ascension	11:43:45.6	Ref. frame	Barycentric	
		00:00:00			
	Declination	-1:16:36.0	Velocity	0	
00:00:00					
Calibrator	No				
767	Coordinate system	Equatorial	Convention	Optical	targets
	Equinox	J2000			
	Right Ascension	09:27:03.2	Ref. frame	Barycentric	
		00:00:00			
	Declination	-00:52:07.6	Velocity	0	
00:00:00					
Calibrator	No				
768	Coordinate system	Equatorial	Convention	Optical	targets
	Equinox	J2000			
	Right Ascension	09:28:00.3	Ref. frame	Barycentric	
		00:00:00			
	Declination	-00:42:29.8	Velocity	0	
00:00:00					
Calibrator	No				
769	Coordinate system	Equatorial	Convention	Optical	targets
	Equinox	J2000			
	Right Ascension	09:22:20.2	Ref. frame	Barycentric	
		00:00:00			
	Declination	-00:30:58.0	Velocity	0	
00:00:00					
Calibrator	No				

Name	Position		Velocity		Group
770	Coordinate system	Equatorial	Convention	Optical	targets
	Equinox	J2000			
	Right Ascension	09:24:39.1	Ref. frame	Barycentric	
		00:00:00			
	Declination	-00:39:22.3	Velocity	0	
00:00:00					
Calibrator	No				

Sessions:

Name	Session time (hours)	Repeat	Separation	LST minimum	LST maximum	Elevation minimum
HI Observing	4.5	11	0 day	03:49:25	23:30:37	15

Session Constraints:

Name	Scheduling constraints	Comments
HI Observing		

Session Source/Resource Pairs:

Session name	Source	Resource	Time
HI Observing	6	Redshifted HI	4.5 hour
	8		
	19		
	25		
	29		
	36		
	39		
	40		
	394		
	405		
	407		
	412		
	421		
	422		
	438		
	468		
	481		
	483		
	495		
	496		
497			
515			
522			
527			
538			
540			
548			
559			
573			
589			

Session name	Source	Resource	Time
	593		
	603		
	605		
	612		
	613		
	614		
	621		
	623		
	625		
	629		
	659		
	705		
	716		
	722		
	728		
	731		
	741		
	745		
	748		
	750		
	765		
	766		
	767		
	768		
	769		
	770		

Present for observation: no

Staff support: None

Plan of dissertation: no

Technical Justification:

Dates:

NA

Observing time:

We plan to observe each source using position-switching for 20 minutes ON + 20 minutes off. We will be observing at L-band with a total of 100 MHz bandwidth, in dual polarization mode.

Assuming a 20 K system temperature at L-band and smoothing to 9 km/s resolution, the sensitivity calculator yields a sensitivity of 1.2 mJy, which is approximately a factor of 2 better than the ALFALFA extragalactic HI survey.

Mapping:

NA

RFI considerations:

We are observing between 1340 and 1440 MHz. There is thus little expected RFI.

The only significant source of RFI is the GPS NUDET (~1381 MHz). We have existing IDL scripts (which will be adapted to GBT-IDL) for identifying integration-by-integration when that RFI is present, and will remove it as necessary.

Overhead:

The start of each session will have a single flux calibrator, which will be observed for 10 minutes, including the time to slew to the calibrator and change receivers to L-band.

Our sources are clustered in a few regions of the sky, and so we can assume a slewing time of 2-3 minutes per source.

For a 4.5 hour session with 40 minutes of integration per source, this would mean roughly 28 minutes of overhead, or 11% of the total session.

Joint considerations:

NA

Novel considerations:

NA

Pulsar considerations:

NA

LST Range Justification:

NA

HI Observations of Very Low Surface Brightness Field Galaxies from the Hyper Suprime-Cam Survey

Overview:

This proposal requests GBT HI spectral observations of 56 very low surface brightness (vLSB; $\bar{\mu}_{\text{eff},g} > 24.3$ mag arcsec $^{-2}$) field galaxies identified in the first 200 deg 2 of the Hyper Suprime-Cam Subaru Strategic Program (HSC-SSP) with the 8.2m Subaru Telescope. The HSC-SSP has uncovered a diverse sample of 781 vLSB galaxies (Greco et al. 2018b) that could probe possible connections between field and cluster populations of vLSB galaxies, as well as constrain cosmological and galaxy formation models. However, optical spectroscopy of these sources is difficult and expensive - currently only eight of these galaxies in low density environments have distance measurements. Thus, *this proposal aims to determine the distances to, and constrain the HI gas contents of, a carefully selected subset of these sources that appear to be in the field, and likely to have HI.* These measurements will help constrain the cosmic number density and formation models for the enigmatic population of vLSB galaxies in low density environments.

The Importance of very Low Surface Brightness Field Galaxies:

Low surface brightness galaxies represent a significant (e.g., McGaugh et al. 1995) and cosmologically important (e.g., O’Neil et al. 1997) part of the galaxy population. While they have been studied for decades (see Bothun et al. 1997 for a review), the detection of a substantial population of physically large red LSB galaxies in dense clusters (van Dokkum et al. 2015) — so-called ultra-diffuse galaxies (UDGs) — has regenerated interest in the extremes of this population. These vLSB, ultra-diffuse sources are remarkable in that they have dwarf-like stellar masses ($\sim 10^7 M_{\odot}$) spread over Milky-Way-like effective radii (>1.5 kpc). A smaller number of “ultra-diffuse” galaxies with similar masses, radii, and surface brightnesses to cluster UDGs have been identified in lower density environments (e.g., Martínez-Delgado et al. 2016; Román & Trujillo 2017). Often these sources are rich in HI (e.g., Leisman et al. 2017; Spekkens et al. 2018), and are bluer than the vLSB galaxies in clusters, and may or may not be physically related to the cluster population.

The mechanism that creates galaxies with such large radii relative to their stellar mass is still a question of intense debate, especially in the field. vLSB sources in groups and clusters may in part result from environmental effects like tidal encounters (e.g., Burkert 2017) or ram pressure stripping (e.g., Yozin & Bekki 2015). But vLSB galaxies in the field likely require an internal mechanism like gas outflows (Di Cintio et al. 2017) or high dark matter angular momentum (Amorisco & Loeb 2016). Moreover, this field population may hold the key to solving famous Λ CDM tensions on small scales (e.g., Papastergis et al. 2015; Giovanelli & Haynes 2015). Likely dark matter dominated, vLSB sources enable the study of dark matter mass distributions to large radii with comparatively little ambiguity from baryons, and their comparative isolation means environmental factors do not complicate their evolutionary history. Yet, constraining the cosmic abundance of the field vLSB population, understanding how it formed, and whether it is connected to the cluster population requires a complete census of vLSB sources.

Existing Catalogs of Field vLSB Galaxies – Potential & Limitations:

HI is an extremely effective way to study vLSB galaxies in the field, since such isolated systems tend to be gas rich. Indeed, Leisman et al. (2017) have identify a sample of 115 isolated “ultra-diffuse,” HI-rich galaxies in the ALFALFA extragalactic HI survey (e.g., Giovanelli et al. 2005, Haynes et al. 2018). However, this work was limited by the shallow survey depth and declination limitations of ALFALFA. Thus, by virtue of their HI selection, these sources tend to be highly gas rich (mean $M_{\text{HI}}/M_{\star}=35$), and not necessarily representative of typical field UDGs.

In contrast, Greco et al. (2018b) carried out a blind optical search for LSB galaxies with the HSC-SSP, finding 781 LSB sources that span a wide range of galaxy colors, central surface brightnesses, morphologies, and environments (left panel of Figure 1). This sample, therefore, has the potential

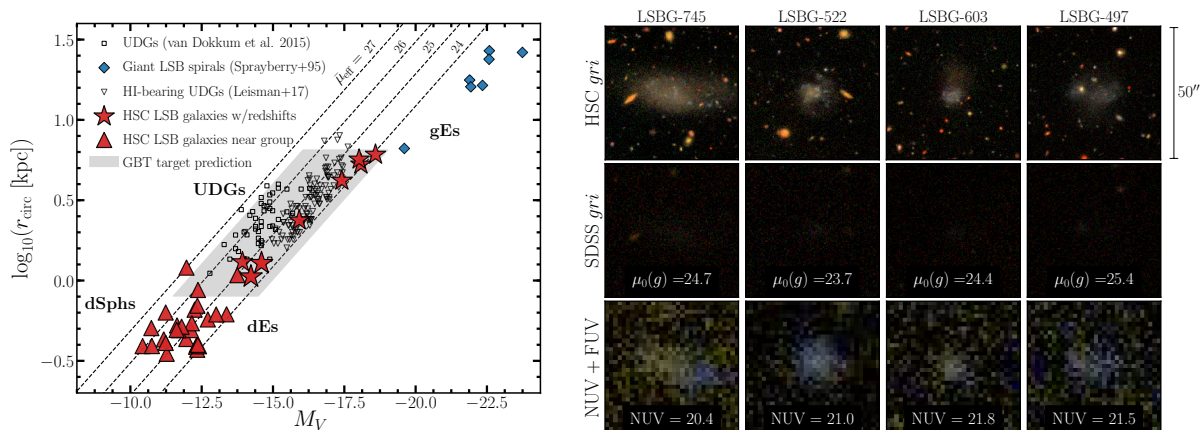


Figure 1: *Left*: Size-luminosity relation for LSB galaxies from the full catalog of Greco et al. 2018b, compared with samples of giant LSB spirals, and UDGs. Stars show galaxies with archival or recently acquired (Greco et al. 2018c) spectroscopic redshifts, and large triangles show galaxies that are projected near a low- z galaxy group. We expect the sources we propose to observe to populate the region shown in grey. *Right*: HSC, SDSS, and GALEX images of example GBT targets from this proposal. HI observations will provide distances, HI gas content, and projected rotational velocities for these extreme sources, placing them on the relation in the left panel.

to connect LSB galaxies across gas fractions and halo environments. However, while this and other optically selected samples avoid the limitations of HI selection, *their analysis is severely limited by the lack of spectroscopic, and thus distance, information.* Indeed, only six archival spectroscopic redshifts exist for the Greco et al. (2018b) catalog (three of which come from ALFALFA, which covers $\sim 40\%$ of the HSC-SSP footprint). Additionally, new deep optical spectroscopic observations have shown two HSC-SSP vLSB sources to be very isolated (~ 2 Mpc from a massive host) ultra-diffuse dwarfs beyond the Local Volume (Greco et al. 2018c). However, such observations are expensive, making it difficult to obtain distances for a significant fraction of these objects. Without distances, disentangling diffuse Milky Way cirrus, nearby dwarfs, or more distant “ultra-diffuse galaxies” is impossible (e.g. Greco et al. 2018a).

Primary Science Objectives of GBT Observations – Distances & Gas Content:

Thus, we propose a pilot HI survey of potential field galaxies from the HSC LSB galaxy catalog. We focus on blue vLSB sources (right panel of Figure 1), which we expect to detect at approximately 2x the depth of ALFALFA (Figure 2). We have two primary observational goals:

- 1) *To obtain redshift distances for a significant number of optically selected field vLSB galaxies.* The clustering-based (statistical) redshift distribution of the LSB galaxies that meet our selection criteria (Greco et al., in prep) suggests that $\sim 73\%$ of our sample falls within 100 Mpc (and $\sim 85\%$ has $z < 0.05$; see Figure 2). Thus, for sources with modest gas fractions, the most economical method of estimating their distances is by determining their redshifts using moderate depth HI observations.

Distance measures will constrain the galaxies’ physical properties, including their baryonic masses and physical extents, and allow for measurements of their environments. Such properties, in turn, will allow for direct comparisons with those of other samples of vLSB galaxies. We estimate below that we will detect and measure HI redshifts and thus obtain distance estimates for $\sim 60 - 70\%$ of our proposed sources. This would mean an additional $\sim 33 - 35$ sources, $>4x$ the current sample. Even with a lower detection rate, these observations will yield a significant increase in the number of known distances in the HSC-SSP vLSB sample.

- 2) *To understand the gas contents of field vLSB galaxies.* For detected sources, we will be

able to directly measure the HI mass and HI gas fractions of the galaxies, which in turn can help constrain their star formation laws. Additionally measurements of the HI line widths of detected sources will allow for rough constraints on their rotation and dark matter content.

For sources without detections, we will still be able to place significant upper limits on the gas fractions in those sources, probing the gas fraction distribution of vLSB field galaxies. Targeted observations of optically selected samples (e.g., Catinella et al. 2010) have shown that surface brightness creates a fundamental plane with color and gas fraction, such that lower surface brightness sources tend to have higher gas fractions, and Huang et al. (2012) suggest a similar result for HI selected samples, with an offset in gas fraction of ~ 0.3 dex. However, this relation is poorly constrained for vLSB galaxies; Papastergis et al. (2017) suggest that perhaps vLSB galaxies have a bimodal gas fraction based on Effelsburg observations of four optically detected field ultra-diffuse galaxies, but are limited by their small sample size. Here a sample of 56 sources will provide a far better probe of vLSB galaxy gas fractions.

Moreover, as future optical catalogs uncover ever larger samples of vLSB galaxies, understanding the detection fraction as a function of color, and whether the scaling relations at higher surface brightness hold for these samples will be critical for future, larger follow up campaigns to obtain distances to these enigmatic and important sources.

Sample Selection and Predicted Detection Statistics:

Selecting a sample of field vLSB galaxies from the HSC-SSP catalog is complicated by the fact that without distances, environmental estimates are limited to projection on the sky. However, field galaxies tend to be the bluest galaxies in the sample, and also those with the most HI (e.g., Papastergis et al. 2013). Thus, we select blue vLSB galaxies with $g-r < 0.4$, a compromise between probing a wide parameter space, and increasing the likelihood of a source being in the field and having detectable HI. To guard against confusion and for clean detection statistics (given the 9' GBT beam at 21 cm), we remove sources that are $< 4.5'$ from any ALFALFA source or from any galaxy in the NASA-Sloan Atlas with $M_\star > 10^{10} M_\odot$ in the region not covered by ALFALFA. We limit the catalog to sources visible to GBT for a significant period during the spring semester (6 hr $< \text{RA} < 18$ hr), and enforce a central surface brightness cut ($\mu_0(g) > 23.0$ mag $''^{-2}$) in addition to the effective surface brightness selection of the initial HSC-LSB catalog, removing nucleated sources from the sample. Finally, we ensure we are looking at only the most diffuse local sources by placing a minimum radius cut $r_e > 4''$. These cuts leave 62 galaxies. We additionally remove six face-on spirals that appear to be background galaxies, for a final sample of 56 galaxies.

We then estimate the HI gas fractions of our sources using standard relations with color and surface brightness for optically selected sources (Catinella et al. 2010), and use these to estimate the HI masses of our sources at 100 Mpc (the high end of our expected distances - see Figure 2). Our chosen threshold of 1.2 mJy/ channel gives a 5σ HI mass detection threshold of $\log(M_{\text{HI}}/M_\odot) = 8.78$ at 100 Mpc for sources with a velocity width of 100 km s^{-1} (or 8.62 for $W_{50} = 50 \text{ km s}^{-1}$; the median ALFALFA velocity width for our expected HI masses is $\sim 100 \text{ km s}^{-1}$, but Leisman et al. (2017) find narrower velocity widths for vLSB sources). If the galaxies fall on the typical scaling relations, then we expect a detection rate between 53% (assuming an average line width of 100 km s^{-1}), and 77% (assuming 50 km s^{-1}), given our expected distances. *Given the high likelihood these are low-z sources, a low detection fraction will imply very different gas scaling relations than those inferred from known samples.* We note that these scaling relations predict ~ 4 ALFALFA detections in the portion of the HSC-SSP field covered by ALFALFA, consistent with the 3 ALFALFA detections. We further note that 87% of the sources in our sample are detected in GALEX observations (MIS and AIS). This suggests recent star formation, which is usually accompanied by HI, consistent with our predictions from scaling relations.

Observing request:

We request a total of 49.5 hours of observing time, including overhead to observe 56 targets which are good candidates for detection in HI. We will observe using a standard total-power position-

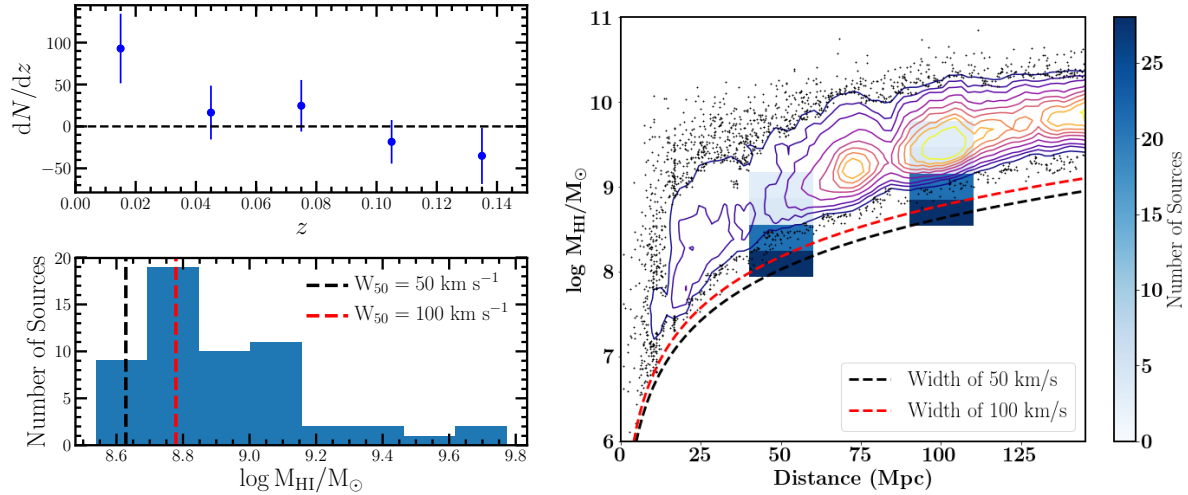


Figure 2: *Top Left*: Clustering-based redshift distribution of galaxies that meet our selection criteria (Greco et al., in prep.), suggesting that $\sim 85\%$ of our sample has $z < 0.05$. *Bottom Left*: The predicted HI mass distribution of our proposed targets based on scaling relations from Catinella et al. 2010. The 5σ detection limits (assuming $W_{50} = 50$ and 100 km s^{-1}) are indicated with a vertical dashed lines. *Right*: Spauhnauer diagram of sources in the ALFALFA survey (contours and dots), with our proposed 5σ detected thresholds (dashed lines). The blue bars show the predicted HI masses of our sample at two different distances, demonstrating that we expect to find most sources above our detection threshold, but but at lower masses than ALFALFA. Thus, a modest increase in depth should result in a dramatic increase in detections (note: the HSC-SSP field covers only $\sim 1\%$ of the ALFALFA area, thus the 3 existing ALFALFA detections are consistent with this prediction).

switching mode, observing in iterative 5 minute ON-OFF pairs until the source is detected or we total 20 minutes ON and 20 minutes OFF per source yielding a 1.2 mJy rms in 9 km s^{-1} channels. Including overhead, we thus estimate a rate of ~ 5 sources per 4.5 hour observing block. Since over half of the HSC-SSP footprint is outside the Arecibo declination range, and the rest is at high zenith angles for Arecibo, these observations are best executed with the GBT.

Undergraduate students and faculty (see <http://egg.astro.cornell.edu/alfalfa/ugradteam/gbt.uatlist.html>) in the Undergraduate ALFALFA Team (UAT) will be heavily involved in this program, conducting observations remotely and analyzing data. We request 4 hours on Friday, June 28, when UAT members will be onsite at Green Bank for the annual UAT workshop. Other observations can be performed in any operational weather conditions.

References:

- Amorisco & Loeb 2016, MNRAS, 459, L51
Bothun et al. 1997, PASP, 109, 745
Burkert 2017, ApJ, 838, 93
Catinella et al. 2010, MNRAS, 403, 683
Di Cintio, et al. 2017, MNRAS, 466, L1
Giovanelli et al. 2005, AJ, 130, 2598
Giovanelli & Haynes 2015, A&ARv, 24, 1
Greco et al. 2018a, PASJ, 70, 19
Greco et al. 2018b, ApJ, 857, 104
Greco, et al. 2018c, arXiv:1805.04118
Haynes et al. 2018, ApJ, 861, 49
Huang et al. 2012, ApJ, 756, 113
Leisman et al. 2017, ApJ, 842, 133
Martinez-Delgado et al. 2016, AJ, 151, 96
McGaugh et al. 1995, AJ, 110, 573
O’Neil et al. 1997, AJ, 114, 2448
Papastergis et al. 2013, ApJ, 776, 43
Papastergis, et al. 2015, A&A, 574A, 13
Papastergis, et al. 2017, A&A, 601L, 10
Roman & Trujillo 2017, MNRAS, 468, 703
Spekkens et al. 2018, ApJ, 855, 28
Sprayberry et al. 1995, AJ, 109, 558
van Dokkum et al. 2015, ApJ, 798, 45
Yozin & Bekki 2015, MNRAS, 452, 937